



Universiteit
Leiden
The Netherlands

Advanced computed tomography for cardiac applications : from cardiovascular diagnosis to clinical management

Graaf, F.R. de

Citation

Graaf, F. R. de. (2012, December 2). *Advanced computed tomography for cardiac applications : from cardiovascular diagnosis to clinical management*. Retrieved from <https://hdl.handle.net/1887/18438>

Version: Corrected Publisher's Version

License: [Licence agreement concerning inclusion of doctoral thesis in the Institutional Repository of the University of Leiden](#)

Downloaded from: <https://hdl.handle.net/1887/18438>

Note: To cite this publication please use the final published version (if applicable).



5

Diagnostic Accuracy of 320-Row Multi-Detector Computed Tomography Coronary Angiography to Non-Invasively Assess In-Stent Restenosis

FR de Graaf, JD Schuijf, JE van Velzen, LJ Kroft, A de Roos, JHC Reiber, A Sieders, F Spanó, JW Jukema, MJ Schaliq, EE van der Wall, JJ Bax

Invest Radiol. 2010;45:331-40

ABSTRACT

Percutaneous coronary intervention with stent implantation is routinely performed to treat patients with obstructive coronary artery disease (CAD). However, thus far, non-invasive assessment of in-stent restenosis has been challenging. Recently, 320-row multi-detector computed tomography coronary angiography (CTA) was introduced, allowing volumetric image acquisition of the heart in a single heart beat or gantry rotation. The aim of the present study was to evaluate the diagnostic performance of 320-row CTA in the evaluation of significant in-stent restenosis. Invasive coronary angiography (ICA) served as the standard of reference, using a quantitative approach. The population consisted of patients with previous coronary stent implantation who were clinically referred for cardiac evaluation due to recurrent chest pain and who underwent both CTA and ICA. CTA studies were performed using a 320-row CTA scanner with 320 detector-rows, each 0.5 mm wide, and a gantry rotation time of 350 ms. Tube voltage and current were adapted to body mass index (BMI) and thoracic anatomy. The entire heart was imaged in a single heart beat, with a maximum of 16 cm cranio-caudal coverage. During the scan, the ECG was registered simultaneously for prospective triggering of the data. First, CTA stent image quality was assessed using a 3-point grading scale: 1: good image quality, 2: moderate image quality, 3: poor image quality. Subsequently, the presence of in-stent restenosis was determined on a stent and patient basis by a blinded observer. Significant in-stent restenosis was defined as $\geq 50\%$ luminal narrowing in the stent lumen and/or the presence of significant stent edge stenosis (significant stenosis < 5 mm from the stent edge). Overlapping stents were considered to represent a single stent. Results were compared to ICA using quantitative coronary angiography (QCA). In addition, CTA stent image quality was related to stent characteristics and heart rate during CTA image acquisition. The population consisted of 53 patients (37 men, mean age of 65 ± 13 years) with a total of 89 stents available for evaluation. ICA identified 12 stents (13%) with significant in-stent restenosis. After the exclusion of 7 stents (8%) due to non-diagnostic CTA stent image quality, sensitivity, specificity, positive and negative predictive values were 92%, 91%, 65% and 98%, respectively on a stent basis. Five CTA studies (9%) were of non-diagnostic quality for the evaluation of in-stent restenosis. Sensitivity, specificity, positive and negative predictive values were 100%, 92%, 79% and 100%, respectively on a patient level. Stent diameter < 3 mm as well as stent strut thickness ≥ 140 μm were associated with decreased CTA stent image quality. Heart rate during CTA acquisition and stent overlap were not associated with image degradation. The present results show that 320-row CTA allows accurate non-invasive assessment of significant in-stent restenosis. However, stents with a large diameter and thin struts allowed better in-stent visualization than stents with a small diameter or thick struts. As a result, non-invasive assessment of in-stent restenosis using CTA may be an attractive and feasible alternative particularly in carefully selected patients.

INTRODUCTION

Coronary artery disease (CAD) is the leading cause of morbidity and mortality in industrialized society. To treat patients with obstructive atherosclerosis, percutaneous coronary intervention with stent implantation is routinely performed, which considerably reduces the rate of restenosis as compared to balloon angioplasty.¹ Nevertheless, also in patients treated with coronary stent implantation, a risk of in-stent restenosis remains.² Specifically, stent implantation may be followed by early in-stent thrombosis³ or later occurring in-stent restenosis due to neointimal hyperplasia.⁴ Early detection and treatment of in-stent restenosis is of vital importance, as it may help reduce morbidity and mortality. Considering an increasingly growing number of patients with coronary stent implantation, in combination with the potential risk of in-stent restenosis, a non-invasive approach for the detection of in-stent restenosis would be desirable.

With the introduction of multi-detector computed tomography coronary angiography (CTA) the non-invasive assessment of the coronary artery tree has become feasible.^{5,6} Although early 4-row CTA systems did not yet enable the evaluation of stented coronary segments,⁷ with improved spatial and temporal resolutions of 16-row^{8,9} and 64-row systems^{10,11} the assessment of in-stent restenosis became feasible. In spite of increased temporal and spatial resolution of 64-row CTA, a proportion of stents remained uninterpretable, predominantly due to cardiac motion artifacts as well as high-density artifacts caused by the metallic stent struts.¹²

Recently, a new generation of CTA scanners became available with 320 simultaneous detector-rows each 0.5 mm wide and increased temporal resolution as compared to most of the previous scanner generations.^{13,14} Due to superior cranio-caudal coverage up to 16 cm, these systems allow a volumetric scanning approach, covering the entire heart in a single gantry rotation or heart beat. Single heart beat image acquisition has some advantages over scanning techniques requiring multiple heart beats. Firstly, the reduced scan time shortens the time of breath-hold as well as lowering the amount of contrast injection. Moreover, volumetric scanning decreases patient radiation exposure by eliminating helical oversampling¹⁵ and furthermore eliminates the problem of stair-step artifacts, observed in helical or step-and-shoot scanning techniques. Although the diagnostic accuracy of 320-row CTA in the anatomic assessment of significant CAD has been recently reported,^{16,17} no information is currently available on the evaluation of patients with previous stent implantation. The purpose of the present study, therefore, was to evaluate the diagnostic accuracy of 320-row CTA in the evaluation of significant in-stent restenosis. Invasive coronary angiography (ICA) served as the standard of reference, using a quantitative approach. A second purpose of the study was to assess

CTA stent image quality versus stent characteristics and heart rate during CTA image acquisition.

MATERIALS AND METHODS

The population consisted of patients with previous coronary stent implantation who were clinically referred for cardiac evaluation due to recurrent chest pain and who underwent both CTA and ICA. Exclusion criteria for CTA examination were: 1) (supra) ventricular arrhythmias, 2) renal failure (glomerular filtration rate < 30 ml/min), 3) known allergy to iodine contrast material, 4) severe claustrophobia, 5) pregnancy. Diagnostic ICA served as the standard of reference using quantitative coronary angiography (QCA). Both examinations were performed within three months of each other. No interventions or changes in the clinical condition of the patients occurred between the examinations.

CTA Data Acquisition

CTA studies were performed using a 320-row CTA scanner (Aquilion ONE, Toshiba Medical Systems, Otawara, Japan) with 320 detector-rows (each 0.5 mm wide) and a gantry rotation time of 350 ms, translating into a temporal resolution of 175 ms for half scan reconstructions. Metoprolol was administered orally (50-100 mg depending on heart rate) one hour prior to data acquisition to patients with a heart rate > 65 beats/min, unless contraindicated. The entire heart was imaged in a single heart beat, with a maximum of 16 cm cranio-caudal coverage. During the scan, the ECG was registered simultaneously for prospective triggering of the data. The phase window was set at 65-85% of R-R interval in patients with a heart rate between 60 and 65 beats/min, and 75% of R-R interval in patients with stable heart rate < 60 beats/min. In patients requiring LV function measurements, prospective ECG triggered dose modulation was used. Using prospective dose modulation, an entire cardiac cycle was scanned attaining maximal tube current during the pre-defined interval. The tube current outside of the pre-defined interval was 25% of the maximal tube current. In patients with a heart rate > 65 beats/min, CTA acquisition was performed during multiple heart beats (typically two).

Tube voltage and current were adapted to body mass index (BMI) and thoracic anatomy. Tube voltage was 100 kV (BMI < 23 kg/m²), 120 kV (BMI 23-35 kg/m²) or 135 kV (BMI ≥ 35 kg/m²) and maximal tube current was 400-580 mA (depending on body weight and thoracic anatomy). A tri-phasic injection of 60-80 ml intra-venous non-ionic contrast media (Iomeron 400; Bracco, Milan, Italy) was performed in the antecubital vein. First, 50-70 ml (depending on body weight) of contrast media was administered at a flow rate of 5.0 or 6.0 ml/s, followed by 20 ml of 50% contrast/saline mix. Subsequently, a saline flush

of 25 ml was administered at a flow rate of 3.0 ml/s. In order to synchronize the arrival of the contrast media and the scan, bolus arrival was detected using a automated peak enhancement detection technique¹⁸ in the left ventricle. CTA was automatically initiated when a threshold of +180 Hounsfield Units was reached. All images were acquired during an inspiratory breath-hold of approximately 5 seconds. During the CTA examination mean heart rate was 59 ± 12 beats/min (range: 41-99 beats/min). An initial data set was reconstructed at 75% of R-R interval, with a slice thickness of 0.50 mm and a reconstruction interval of 0.25 mm. If multiple phases were obtained, additional reconstructions were explored in case of motion artifacts, in order to obtain images with the least motion artifacts. For processing and evaluation, images were transferred to a remote workstation with dedicated CTA analysis software (Vitrea FX 1.0, Vital Images, Minnetonka, MN, USA). The average investigation time for the CTA study was approximately 20 minutes. CTA investigations were completed successfully in all patients without complications.

Radiation dose was quantified with a dose-length product conversion factor of 0.014 mSv/(mGy×cm) as previously described.¹⁹ In patients who were scanned full dose at 75% of R-R interval, estimated mean radiation dose was 3.2 ± 1.1 mSv. In patients who were scanned full dose at 65-85% of R-R interval, estimated mean radiation dose was 7.1 ± 1.7 mSv. In patients requiring LV function measurements dose modulated scans were performed with an estimated mean radiation dose of 10.7 ± 3.6 mSv. In patients in whom CTA image acquisition was performed during multiple heart beats mean estimated radiation dose was 16.7 ± 6.3 mSv.

CTA Image Analysis

CTA image analysis was performed by 2 observers in consensus, experienced in the evaluation of CTA and unaware of the results of ICA. Stent location in the coronary artery tree was assessed in a standardized manner by dividing the coronary artery tree into 17 segments according to a modified American Heart Association classification.²⁰ The presence of in-stent restenosis was analyzed on a stent and patient level. Overlapping stents were considered to represent a single stent, as overlap hampers individual stent assessment. When multiple reconstructions from different cardiac phases were available, the reconstruction with the best image quality was evaluated. In addition, different window settings were used for optimal stent assessment. Furthermore, a second set was reconstructed using a sharp convolution kernel (FC50) allowing more clear visualization of in-stent lumen (Figure 1, panel C and Figure 2, panel B). The original transaxial slices were visually examined assisted by curved multiplanar reconstructions. First, stent image quality was assessed, by evaluating in-stent lumen visibility, using a 3-point grading scale: 1: good image quality (no artifacts), 2: moderate image quality (moderate image degradation), 3: poor image quality (severe image degradation). Subsequently, each

stent was evaluated for the presence of significant in-stent restenosis. Significant in-stent restenosis was defined as a darker eccentric or concentric rim between the stent and the enhanced vessel lumen, with a lumen reduction $\geq 50\%$ and/or the presence of significant stent edge stenosis (significant stenosis < 5 mm from the stent edge). In addition, run-off distal to the stent was evaluated, and reduced run-off distal to the stent was judged to be suggestive of in-stent restenosis. Of note, the presence of run-off distal to the stent was not used as an indication for the absence of significant in-stent restenosis, as collateral filling of distal segments is possible. A stent was considered to be occluded when the contrast enhancement in the lumen inside the stent was lower than in the contrast-enhanced vessel before the stent. In addition the absence of run-off

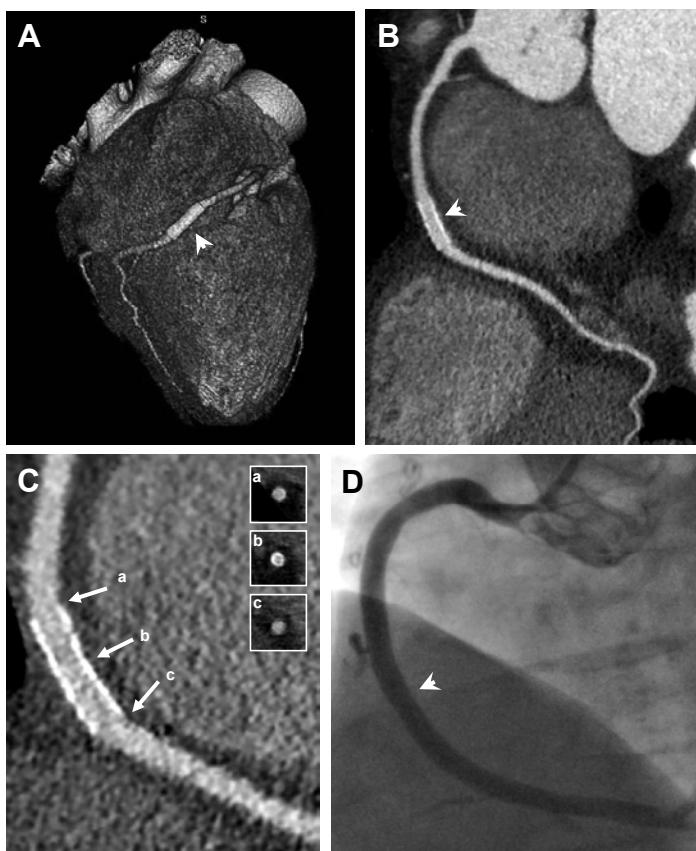


Figure 1. 320-row CTA of a patent stent (Ultra, 4.5 mm x 18 mm) in the RCA of a 60 year-old male patient. Panel A shows a three-dimensional volume rendered reformation of the heart showing an overview of the RCA with a stent (arrowhead) in segment 2. Panel B depicts a curved multiplanar reconstruction of the RCA showing a patent stent (arrowhead). Panel C shows a curved multiplanar reconstruction using a sharp convolution kernel. In the upper right-hand corner, transverse sections of the stent and both stent edges (arrows) help confirm the absence of in-stent hyperplasia. An invasive coronary angiogram in panel D confirmed the observation.

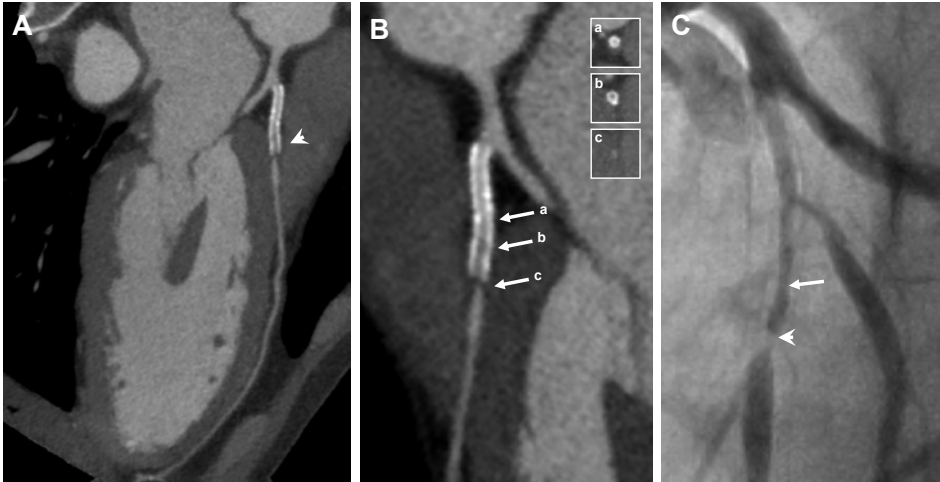


Figure 2. 320-row CTA reveals patency of three adjacent, partially overlapping drug-eluting stents (from proximal to distal: Endeavor, 4.0 mm x 24 mm; Promus, 4.0 mm x 23 mm; Endeavor 4.0 mm x 15 mm) in a venous bypass graft of a 86 year-old male patient. Multiplanar reconstructions in panel A and panel B (using a sharp convolution kernel) reveal stent patency (arrowheads). An invasive angiogram (Panel C) confirms the absence of significant in-stent hyperplasia (arrowhead).

at the distal end of the stent was judged to be an indication of stent occlusion. Finally patient based analysis was performed. In patients with a single uninterpretable stent, the entire CTA was deemed non-diagnostic. However, in patients with multiple stents, in case one stent was uninterpretable, an intention to diagnose strategy was applied. If more than one stent in a single patient with multiple stents was deemed uninterpretable, the entire CTA was considered to be of non-diagnostic image quality. Figures 1 and 2 provide examples of a patent stent in the right coronary artery (RCA) and a patent stent in a venous bypass graft, respectively. Figure 3 depicts a stent in the left anterior descending (LAD) artery with significant in-stent restenosis.

ICA Analysis

ICA was performed using standardized techniques and all angiograms were assessed by an experienced observer blinded to the CTA data. First, angiograms were examined prior to contrast injection, to localize the stent in the coronary artery tree. Similar to CTA analysis, the available coronary segments were identified on the basis of the American Heart Association guidelines. Subsequently, all stents were visually classified as normal (no atherosclerosis or minor wall irregularities with $\leq 20\%$ luminal narrowing) or abnormal (presence of stenosis with $> 20\%$ luminal narrowing). All stents visually scored as abnormal were quantified using a dedicated and validated QCA software package (QAngioXA 6.0, CA-CMS, Medis Medical Imaging Systems, Leiden, the Netherlands). Each stent was evaluated for the presence of significant in-stent restenosis (defined as

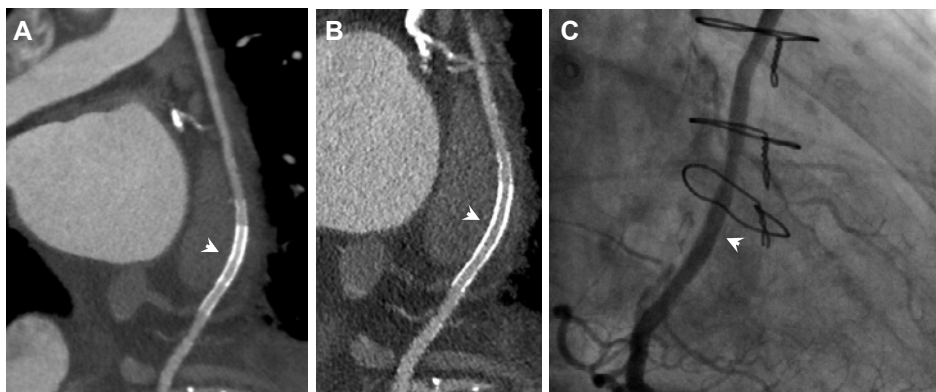


Figure 3. 320-row CTA demonstrates in-stent restenosis in a drug-eluting stent (Endeavor, 2.75 mm x 24 mm) placed in the proximal LAD of a 62 year-old male patient. A curved multiplanar reconstruction in panel A shows significant in-stent restenosis (arrowhead). In panel B, an enlarged curved multiplanar reconstruction is shown. In the upper right-hand corner three transverse sections of the stent and distal stent edge are shown, revealing low-attenuating neointimal hyperplasia corresponding to a severe lesion in the distal stent lumen (arrow b) and a subtotal stenosis at the distal stent-edge (arrow c). Panel C shows an invasive coronary angiogram confirming both findings (arrow and arrowhead).

luminal diameter reduction of $\geq 50\%$ on QCA and/or the presence of significant stent edge stenosis) in the angiographic view with most severe luminal narrowing.

Statistical Analysis

The presence of in-stent restenosis was analyzed on stent and patient level. Sensitivity, specificity, positive and negative predictive values (including 95% confidence interval [CI]) for the detection of significant in-stent restenosis were calculated, using coronary CTA in combination with QCA. In an initial analysis, the diagnostic accuracy was determined excluding stents or patients of non-diagnostic CTA image quality. In a subsequent analysis, non-diagnostic stents or patients were included in the analysis, and were considered positive ($\geq 50\%$ luminal narrowing). Furthermore, percentages of poor, moderate and good CTA stent image quality were compared for small (< 3 mm) vs. large (≥ 3 mm) diameter stents, and thin (< 140 μm) vs. thick (≥ 140 μm) stent struts. In addition, CTA stent image quality was related to stent characteristics and heart rate during CTA image acquisition. Continuous data were expressed as mean \pm standard deviation (SD). Statistical analyses were performed using SPSS software (version 16.0, SPSS Inc., Chicago, Illinois). A value of $p < 0.05$ was considered statistically significant.

RESULTS

Patient Characteristics

The population consisted of 53 symptomatic patients with a total of 121 stents (median 2, range 1-8). An overview of the main clinical characteristics is given in Table 1. In short, 37 men and 16 women, with a mean age of 65 ± 13 years, were included. The mean interval between coronary stent implantation and ICA was 19.3 ± 26.7 months.

Table 1. Clinical characteristics (n=53)

Age (years)	65 ± 13
Men / women	37 / 16
Interval between coronary stent implantation and ICA (months)	19.3 ± 26.7
BMI (kg/m ²)	27 ± 3
Family history of CAD	16 (30%)
Diabetes	12 (23%)
Hypertension	43 (81%)
Hypercholesterolemia	45 (85%)
Current smoker	13 (25%)
Previous myocardial infarction	28 (53%)
Previous coronary artery bypass grafting	8 (15%)

Stent Characteristics

A total of 121 stents were available for assessment on ICA. The following stent types were evaluated: Promus (Boston Scientific, Boston, Massachusetts), Endeavor (Medtronic, Minneapolis, Minnesota), Cypher (Cordis Corp., Johnson & Johnson, Miami, Florida), Vision (Guidant, Santa Clara, California), AVE S7 (Medtronic), Driver (Medtronic), Janus (Sorin Group, Milano, Italy), AVE (Medtronic), BxSonic (Cordis Corp.), Chrono (Sorin Group), Orbus (OrbusNeich, Hoevelaken, the Netherlands), R-stent (OrbusNeich), Titan (Hexacath, Rueil-Malmaison, France) and Ultra (Abbott Vascular, Ontario, Canada). In 8 stents the stent type could not be retrieved.

Mean stent diameter was 3.2 ± 0.4 mm (range 2.5-4.5) and 24 stents had a diameter below 3 mm. Mean stent length was 17.8 ± 6.5 mm (range 8.0-33.0). Of 121 stents 63 stents (52%) were available without overlap. However, 49 stents (40%) were partially overlapping and 10 stents (8%) were entirely overlapping (due to stent implantation inside another stent after previous in-stent restenosis). As overlapping stents were considered a single stent, a total of 89 stents were available for evaluation. The sites of stent implantation were the following: 35 stents (39%) were located in the RCA, 29 stents (33%) were located in the LAD artery, 24 stents (27%) were located in the left circumflex coronary (LCx) artery, and one stent (1%) was located in a venous bypass graft supplying the obtuse marginal branch and the posterior descending artery (Figure 2).

Coronary Stent Analysis

In a total of 89 stents available for evaluation, ICA identified 12 stents with significant in-stent restenosis (10 non-occluded stents with $\geq 50\%$ in-stent restenosis and 2 occluded stents). However, out of 89 stents identified on ICA, 7 stents (8%) were of non-diagnostic CTA stent image quality. Reasons for non-diagnostic CTA stent image quality were high-density artifacts due to stent material ($n=6$) or severe calcifications ($n=1$). Accordingly, in an initial analysis excluding non-diagnostic stents, 82 stents were available for evaluation on CTA. A total of 11 stents with significant in-stent restenosis were correctly identified on CTA, including both occluded stents. In addition, 64 patent stents were correctly identified by CTA, while the grade of in-stent restenosis was overestimated in 6 stents. Furthermore, one stent with significant luminal narrowing on ICA was underestimated on CTA. Accordingly, sensitivity, specificity, positive and negative predictive values to detect significant in-stent restenosis were 92%, 91%, 65% and 98%, respectively. This resulted in a diagnostic accuracy of CTA in the detection of significant in-stent restenosis of 91%.

In a second analysis, non-diagnostic stents were included and considered positive (for the presence of significant in-stent restenosis). Although the sensitivity and negative predictive value were unchanged, the overall diagnostic accuracy of CTA in the detection of significant in-stent restenosis decreased to 84%. More detailed information is provided in Table 2.

Table 2. Diagnostic accuracy of 320-row CTA for the detection of significant in-stent restenosis.

	Stent Based Analysis	Patient Based Stent Analysis
Excluding non-diagnostic stents and patients		
Non-diagnostic	7/89, 8%	5/53, 9%
Sensitivity	11/12 (92%, 76%-100%)	11/11 (100%)
Specificity	64/70 (91%, 85%-98%)	34/37 (92%, 83%-100%)
PPV	11/17 (65%, 42%-87%)	11/14 (79%, 57%-100%)
NPV	64/65 (98%, 95%-100%)	34/34 (100%)
Diagnostic Accuracy	75/82 (91%, 85%-98%)	45/48 (94%, 87%-100%)
Including non-diagnostic stents and patients		
Sensitivity	11/12 (92%, 76%-100%)	11/11 (100%)
Specificity	64/77 (83%, 75%-91%)	34/42 (81%, 69%-93%)
PPV	11/24 (46%, 26%-66%)	11/19 (58%, 36%-80%)
NPV	64/65 (98%, 95%-100%)	34/34 (100%)
Diagnostic Accuracy	75/89 (84%, 77%-92%)	45/53 (85%, 75%-95%)

Data are absolute values used to calculate percentages. Data in parenthesis are percentages with 95% CI.

Patient Based Stent Analysis

In a total of 53 patients with previous coronary stent implantation, 9 patients were diagnosed with non-occlusive in-stent restenosis and 2 patients had an occluded stent. However, in 5 out of 53 patients (9%) the CTA study was of non-diagnostic quality for the evaluation of in-stent restenosis. Therefore, initial analysis was performed in 48 patients. CTA correctly identified all 11 patients with significant in-stent restenosis. However, in one of these patients, CTA underestimated the degree of restenosis in a stent in the LAD while a lesion in a stent in the LCx was incorrectly deemed obstructive. In all other stents, the presence of significant in-stent restenosis was correctly identified by CTA. Furthermore, in 34 patients in which CTA determined the absence of significant in-stent restenosis, stent patency was confirmed on ICA. However, CTA incorrectly diagnosed 3 patients with significant in-stent restenosis. Consequently, on a patient basis the sensitivity, specificity, positive and negative predictive values to detect significant in-stent restenosis were 100%, 92%, 79% and 100%, respectively. This resulted in a diagnostic accuracy of CTA to detect of significant in-stent restenosis of 94%. In a second analysis, non-diagnostic patients were included and considered positive. The sensitivity and negative predictive values remained unchanged, while the overall diagnostic accuracy decreased to 85%. The diagnostic accuracy of 320-row CTA for the detection of significant in-stent restenosis on a patient basis is listed in Table 2.

320-Row CTA Stent Image Quality

In order to assess the effect of stent characteristics, stent overlap and heart rate during CTA image acquisition on in-stent lumen visibility, CTA stent image quality was assessed for all stents. A total of 47 stents (53%) were of good image quality, 29 stents (33%) were of moderate image quality, and 13 stents (14%) were of poor image quality. In a subanalysis, CTA stent image quality was evaluated according to stent diameter. In stents with a diameter < 3.0 mm, a significant higher percentage of scans were of poor image quality (35%) as compared to stents with a diameter \geq 3.0 mm (9%). Detailed information on the effect of stent diameter on CTA stent image quality is provided in Figure 4.

In a similar fashion, the effect of stent strut thickness on CTA stent image quality was assessed. In stents with a strut thickness < 140 μ m, a significant higher proportion of scans were of good image quality (61%) when compared to stents with a strut thickness \geq 140 μ m (11%). Figure 5 depicts the effect of strut thickness on CTA stent image quality.

Furthermore, the relationship between stent overlap and CTA stent image quality was assessed. No significant difference in CTA stent image quality was observed when comparing stents with and without overlap ($p=0.894$). In stents with and without overlap,

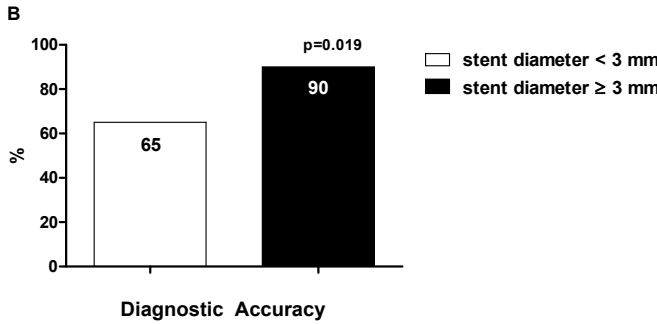
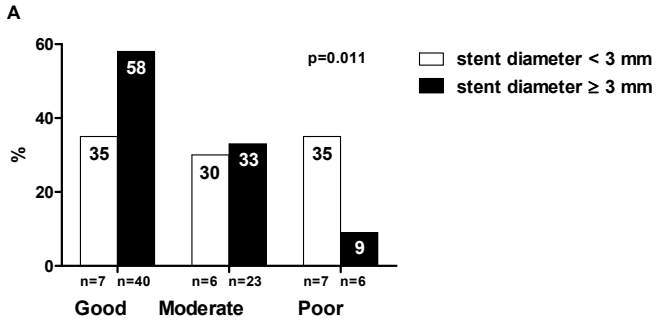


Figure 4. Stent diameter affects CTA stent image quality. CTA stent image quality was significantly better in large diameter stents (≥ 3 mm) as compared to small diameter stents (< 3 mm).

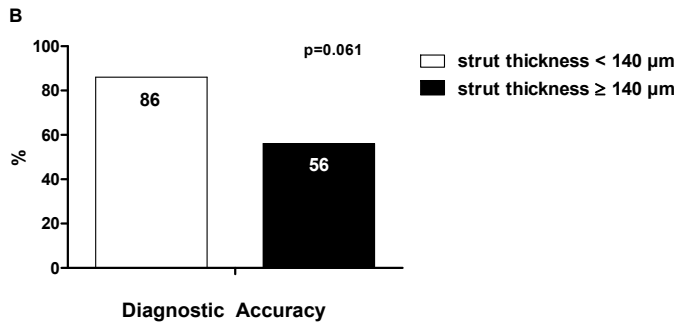
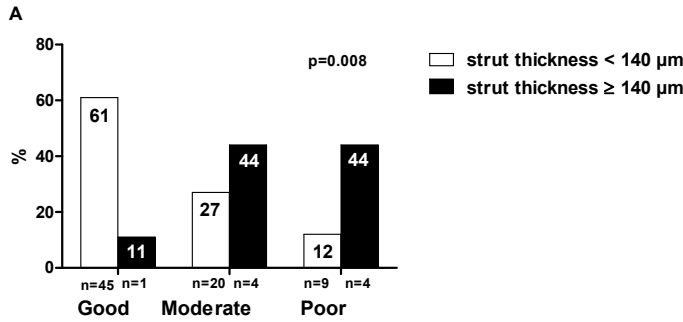


Figure 5. Stent strut thickness affects CTA stent image quality. CTA stent image quality was significantly better in stents with thin struts (< 140 μ m) compared stents with thick struts (≥ 140 μ m).

poor image quality was observed in 15% (4 out of 26 stents) and 14% (9 out of 63 stents), respectively. Similarly, no relationship between heart rate during CTA image acquisition and CTA stent image quality was shown. The mean heart rate during CTA image acquisition in stents of good and moderate image quality was 58 ± 12 beats/min and mean heart rate in stents of poor image quality was 57 ± 8 beats/min ($p=0.825$). Thus, no significant difference in heart rate during CTA acquisition was observed between the two groups.

DISCUSSION

To the best of our knowledge, this is the first report demonstrating the diagnostic accuracy of 320-row CTA for the non-invasive evaluation of significant in-stent restenosis. In the present evaluation, good diagnostic performance of 320-row CTA was demonstrated for the detection of significant in-stent restenosis in 53 patients after coronary stent implantation. Importantly, on a patient basis all patients with significant in-stent restenosis were correctly identified by 320-row CTA, and no patients with significant in-stent restenosis were missed. The excellent negative predictive value suggests that this technique may be especially useful in the exclusion of significant in-stent restenosis. Furthermore, the high sensitivity implies that this technique is also unlikely to miss severe in-stent restenosis. These results are in line with previously published data using 64-row CTA.^{11 21}

Although the diagnostic accuracy of 320-row CTA may be similar to 64-row systems, a volumetric scanning approach has some advantages. First, volumetric scanning enables image acquisition of the entire heart in a single heart beat or gantry rotation.²² This approach reduced total scan time, thereby lowering the amount of contrast injection and decreasing time of breath hold.^{16 17} In addition, single heart beat image acquisition reduces radiation burden by eliminating helical oversampling.^{15 23} Furthermore, the problem of stair-step artifacts, observed in imaging techniques requiring multiple beats to cover the entire heart, is eliminated. As a consequence, 320-row CTA is possibly less prone to artifacts caused by irregular heart rhythm.²⁴ Accordingly, the advantages of volumetric scanning may potentially expand the use of CTA to a broader general population, such as patients with increased heart rate variability.

Stent interpretability

Nevertheless, also using a volumetric scanning approach, 8% of stents were of non-diagnostic CTA image quality in the current report. Previous studies using 64-row CTA reported similar results. A study by Cademartiri et al, in the assessment of in-stent

restenosis in 182 patients, showed that 7.3% of stents were of non-diagnostic CTA image quality, predominantly due to motion artifacts and high density artifacts.¹¹ Likewise, Manghat and colleagues reported non-diagnostic image quality in 9.2% of stents due to severe motion artifacts.²⁵ However, higher rates of non-diagnostic CTA stent image quality have also been described in studies using 64-row CTA.^{26,27} In a study by Rixe and colleagues, only 58% of stents were assessable.²⁷ In another study by Carbone et al, uninterpretable image quality was demonstrated in 28% of stents.²⁸ The wide variation of image interpretability that has been observed in previous studies using 64-row CTA may be largely explained by differences in study inclusion criteria and stent characteristics of the patient population. For instance, in the aforementioned study by Cademartiri and colleagues, a relatively low percentage of uninterpretable stents was observed, as mainly patients with non-overlapping stents were included and stents with a small diameter (≤ 2.5 mm) were excluded from the study.¹¹ Furthermore, patients with a high heart rate and contraindications to beta-blockers were excluded. In contrast, patients with small diameter stents were included in the previously mentioned studies by Rixe et al²⁷ and Carbone et al,²⁸ reporting higher rates of uninterpretable stents. Thus, differences in patient selection and study inclusion criteria may be mostly responsible for the wide variety in rates of stent interpretability previously demonstrated for 64-row CTA.

Stent Characteristics

The current results demonstrated a clear relationship between stent diameter and CTA stent image quality. In stents with a diameter ≥ 3 mm CTA image quality was significantly better than in stents with a diameter < 3 mm. Similar findings have been reported previously by several studies using older scanner generations.²⁹⁻³² This observation may be explained by the fact that metal objects, such as stents, give rise to high-density artifacts, more commonly defined as blooming artifacts, which make the stent struts appear larger than they are in reality. As a consequence, artificial lumen narrowing is observed, obscuring part of the stent lumen. In case of a small diameter stents, high-density artifacts may obscure a large proportion of the stent lumen, thereby rendering the image uninterpretable. Accordingly, also in the present report, small stent diameter hampered stent assessment.

Furthermore, strut thickness may considerably influence CTA stent image quality. The present data showed that significantly more stents with a strut thickness < 140 μm were of diagnostic CTA image quality when compared to stents with a strut thickness struts ≥ 140 μm . The effect of stent strut thickness on CTA image quality has been previously demonstrated.^{21,26,27} Again, the observed effect is related to high-density artifacts, which are more pronounced in objects with higher metallic content, such as stents with thicker struts. Of note, even though stent strut thickness affected stent interpretability, no

significant difference in CTA stent image quality was observed when comparing stents with and without (partial) overlap. These results may be explained by the fact that the majority of overlapping stents were only overlapping to a limited extent. Furthermore, in the present report, overlapping stents did not have complex configurations, such as bifurcational stents, which are more likely to hamper the assessment of in-stent restenosis.³³ Thus, although stent overlap did not seem to hamper stent assessment, stents with thin struts allowed better in-stent visualization when using 320-row CTA.

Heart Rate and Image Quality

Importantly, several studies using older CTA generations refer to motion artifacts as an important reason for CTA stent image degradation.^{21 26-28 31} In the present report, motion artifacts did not seem to play a role in CTA stent image degradation. Furthermore, the current data did not show significant difference in mean heart rate between stents of good and moderate CTA image quality versus stents of poor CTA image quality. These data suggest that, using 320-row CTA, heart rate did not significantly influence CTA stent image quality. A likely explanation for this observation is that, in patients with a heart rate > 65 beats/min, CTA image acquisition was performed during multiple heart beats. Consequently, multi-segment reconstructions were performed, using information from multiple heart beats, still yielding diagnostic image CTA image quality even at increased heart rates. However, it should be noted that multiple heart beat image acquisition is performed at the cost of increased radiation exposure. In addition, 320-row CTA has an increased temporal resolution as compared to most 64-row systems, which decreases the likelihood of image degradation due to cardiac motion. Of note, even higher temporal resolution (83 ms) is obtained with dual-source CTA.³⁴ Nevertheless, 320-row CTA may be less susceptible to image degradation due to heart rate variability, as compared to CTA systems requiring multiple heartbeats to cover the heart. In a recent study by Husmann et al, using prospectively triggered 64-row CTA, it was shown that an important cause of stair-step artifacts was heart rate variability.³⁵ Conversely, single heart beat image acquisition may be less prone to stair-step artifacts, which are an important cause of CTA image degradation.

Clinical Implications

Although good diagnostic accuracy of 320-row CTA has been demonstrated, it is important to realize that optimal CTA stent image quality is only achieved in patients with large stent diameter and thin stent struts. Accordingly, careful patient selection regarding stent type, diameter and strut thickness remains of fundamental importance to optimize the diagnostic performance of 320-row CTA. As a result, the routine use of CTA, i.e. as a gatekeeper for ICA, in symptomatic patients with a history of stent implantation is currently not recommended. Nevertheless, in carefully selected patients,

the non-invasive assessment in-stent restenosis using 320-row CTA may be an attractive alternative to ICA.

Limitations

Several limitations to this study should be addressed. First, CTA is associated with radiation exposure, emphasizing the importance of careful patient selection. Furthermore, visual rather than quantitative in-stent restenosis assessment on CTA was performed. Presently, quantitative approaches to analyze in-stent restenosis on CTA are limited. However, developments of dedicated and validated quantification software for the purpose of CTA are ongoing,³⁶ and a quantitative approach may substantially improve objectivity and reproducibility of the degree of in-stent restenosis observed on CTA. Furthermore, the development of specialized CTA image reconstruction software is in progress, enhancing in-stent visibility, while decreasing image noise.³⁷ Nevertheless, due to artificial luminal narrowing in the presence of metallic stent struts, the evaluation of subtle neointimal hyperplasia remains unlikely in the near future. Future scanning techniques with increased spatial resolution are needed to overcome the problem of artificial luminal narrowing observed in metallic stent struts.

REFERENCES

1. Serruys PW, de Jaegere P, Kiemeneij F et al. A comparison of balloon-expandable-stent implantation with balloon angioplasty in patients with coronary artery disease. Benestent Study Group. *N Engl J Med* 1994;331:489-95.
2. Malenka DJ, Kaplan AV, Lucas FL et al. Outcomes following coronary stenting in the era of bare-metal vs the era of drug-eluting stents. *JAMA* 2008;299:2868-76.
3. Ong AT, Hoyer A, Aoki J et al. Thirty-day incidence and six-month clinical outcome of thrombotic stent occlusion after bare-metal, sirolimus, or paclitaxel stent implantation. *J Am Coll Cardiol* 2005;45:947-53.
4. Morice MC, Colombo A, Meier B et al. Sirolimus- vs paclitaxel-eluting stents in de novo coronary artery lesions: the REALITY trial: a randomized controlled trial. *JAMA* 2006;295:895-904.
5. Vanhoenacker PK, Heijenbrok-Kal MH, Van Heste R et al. Diagnostic performance of multidetector CT angiography for assessment of coronary artery disease: meta-analysis. *Radiology* 2007;244:419-28.
6. Sun Z, Jiang W. Diagnostic value of multislice computed tomography angiography in coronary artery disease: a meta-analysis. *Eur J Radiol* 2006;60:279-86.
7. Kruger S, Mahnken AH, Sinha AM et al. Multislice spiral computed tomography for the detection of coronary stent restenosis and patency. *Int J Cardiol* 2003;89:167-72.
8. Gilard M, Cornily JC, Pennec PY et al. Assessment of coronary artery stents by 16 slice computed tomography. *Heart* 2006;92:58-61.
9. Kefer JM, Coche E, Vanoverschelde JL et al. Diagnostic accuracy of 16-slice multidetector-row CT for detection of in-stent restenosis vs detection of stenosis in nonstented coronary arteries. *Eur Radiol* 2007;17:87-96.
10. van Mieghem CA, Cademartiri F, Mollet NR et al. Multislice spiral computed tomography for the evaluation of stent patency after left main coronary artery stenting: a comparison with conventional coronary angiography and intravascular ultrasound. *Circulation* 2006;114:645-53.
11. Cademartiri F, Schuijff JD, Pugliese F et al. Usefulness of 64-slice multislice computed tomography coronary angiography to assess in-stent restenosis. *J Am Coll Cardiol* 2007;49:2204-10.
12. Kumbhani DJ, Ingelmo CP, Schoenhagen P et al. Meta-analysis of diagnostic efficacy of 64-slice computed tomography in the evaluation of coronary in-stent restenosis. *Am J Cardiol* 2009;103:1675-81.
13. Rybicki FJ, Otero HJ, Steigner ML et al. Initial evaluation of coronary images from 320-detector row computed tomography. *Int J Cardiovasc Imaging* 2008;24:535-46.
14. Hein PA, Romano VC, Lembcke A et al. Initial experience with a chest pain protocol using 320-slice volume MDCT. *Eur Radiol* 2009;19:1148-55.
15. Mori S, Endo M, Nishizawa K et al. Comparison of patient doses in 256-slice CT and 16-slice CT scanners. *Br J Radiol* 2006;79:56-61.
16. Dewey M, Zimmermann E, Deissenrieder F et al. Noninvasive coronary angiography by 320-row computed tomography with lower radiation exposure and maintained diagnostic accuracy: comparison of results with cardiac catheterization in a head-to-head pilot investigation. *Circulation* 2009;120:867-75.
17. de Graaf FR, Schuijff JD, van Velzen JE et al. Diagnostic accuracy of 320-row multidetector computed tomography coronary angiography in the non-invasive evaluation of significant coronary artery disease. *Eur Heart J* 2010;31:1908-15.
18. Cademartiri F, Nieman K, van der Lugt A et al. Intravenous contrast material administration at 16-detector row helical CT coronary angiography: test bolus versus bolus-tracking technique. *Radiology* 2004;233:817-23.

19. Valentin J. Managing patient dose in multi-detector computed tomography(MDCT). ICRP Publication 102. *Ann ICRP* 2007;37:1-79.
20. Austen WG, Edwards JE, Frye RL et al. A reporting system on patients evaluated for coronary artery disease. Report of the Ad Hoc Committee for Grading of Coronary Artery Disease, Council on Cardiovascular Surgery, American Heart Association. *Circulation* 1975;51:5-40.
21. Ehara M, Kawai M, Surmely JF et al. Diagnostic accuracy of coronary in-stent restenosis using 64-slice computed tomography: comparison with invasive coronary angiography. *J Am Coll Cardiol* 2007;49:951-9.
22. Voros S. What are the potential advantages and disadvantages of volumetric CT scanning? *J Cardiovasc Comput Tomogr* 2009;3:67-70.
23. Steigner ML, Otero HJ, Cai T et al. Narrowing the phase window width in prospectively ECG-gated single heart beat 320-detector row coronary CT angiography. *Int J Cardiovasc Imaging* 2009;25:85-90.
24. Pasricha SS, Nandurkar D, Seneviratne SK et al. Image quality of coronary 320-MDCT in patients with atrial fibrillation: initial experience. *AJR Am J Roentgenol* 2009;193:1514-21.
25. Manghat N, Van Lingen R, Hewson P et al. Usefulness of 64-detector row computed tomography for evaluation of intracoronary stents in symptomatic patients with suspected in-stent restenosis. *Am J Cardiol* 2008;101:1567-73.
26. Schuijff JD, Pundziute G, Jukema JW et al. Evaluation of patients with previous coronary stent implantation with 64-section CT. *Radiology* 2007;245:416-23.
27. Rixe J, Achenbach S, Ropers D et al. Assessment of coronary artery stent restenosis by 64-slice multi-detector computed tomography. *Eur Heart J* 2006;27:2567-72.
28. Carbone I, Francone M, Algeri E et al. Non-invasive evaluation of coronary artery stent patency with retrospectively ECG-gated 64-slice CT angiography. *Eur Radiol* 2008;18:234-43.
29. Schuijff JD, Bax JJ, Jukema JW et al. Feasibility of assessment of coronary stent patency using 16-slice computed tomography. *Am J Cardiol* 2004;94:427-30.
30. Gaspar T, Halon DA, Lewis BS et al. Diagnosis of coronary in-stent restenosis with multidetector row spiral computed tomography. *J Am Coll Cardiol* 2005;46:1573-9.
31. Haraldsdottir S, Gudnason T, Sigurdsson AF et al. Diagnostic accuracy of 64-slice multidetector CT for detection of in-stent restenosis in an unselected, consecutive patient population. *Eur J Radiol* 2009.
32. Wolf F, Cademartiri F, Loewe C et al. Evaluation of coronary stents with 64-MDCT: in vitro comparison of scanners from four vendors. *AJR Am J Roentgenol* 2009;193:787-94.
33. Pugliese F, Cademartiri F, Van Mieghem C et al. Multidetector CT for visualization of coronary stents. *Radiographics* 2006;26:887-904.
34. Pugliese F, Weustink AC, Van Mieghem C et al. Dual source coronary computed tomography angiography for detecting in-stent restenosis. *Heart* 2008;94:848-54.
35. Husmann L, Herzog BA, Burkhard N et al. Body physique and heart rate variability determine the occurrence of stair-step artefacts in 64-slice CT coronary angiography with prospective ECG-triggering. *Eur Radiol* 2009;19:1698-703.
36. Marquering HA, Dijkstra J, de Koning PJ et al. Towards quantitative analysis of coronary CTA. *Int J Cardiovasc Imaging* 2005;21:73-84.
37. Min JK, Swaminathan RV, Vass M et al. High-definition multidetector computed tomography for evaluation of coronary artery stents: comparison to standard-definition 64-detector row computed tomography. *J Cardiovasc Comput Tomogr* 2009;3:246-51.